(Supplementary Information)

Bimetallic Nickel-Iridium nanocatalysts for hydrogen generation by decomposition of hydrous hydrazine

Sanjay Kumar Singh and Qiang Xu*

National Institute of Advanced Industrial Science and Technology (AIST), Ikeda, Osaka 563-8577, Japan

* E-mail: q.xu@aist.go.jp

Experimental

General. Commercial chemicals were used as received for catalyst preparation and hydrazine decomposition experiments. Hydrazine monohydrate ($H_2NNH_2 \cdot H_2O$, 99%), sodium borohydride ($NaBH_4$, 99%), hexadecyltrimethyl ammonium bromide (CTAB, 95%), hexadecyltrimethyl ammonium chloride (CTAC, 95%) and $FeCl_2 \cdot 4H_2O$ (95%) were obtained from Aldrich. H_2IrCl_6, $CoCl_2 \cdot 6H_2O$ (99.5%), $NiCl_2 \cdot 6H_2O$ (99.9%), and $CuCl_2$ (95%) were purchased from Wako.

Instrumentation. Mass analysis of the generated gases was performed using a Balzers Prisma QMS 200 mass spectrometer. Powder X-ray diffraction (XRD) studies were performed on a Rigaku RINT-2000 X-ray diffractometer (Cu Kα). UV-visible spectral analyses were performed on Shimadzu UV-2550 spectrophotometer. Scanning electron microscope (SEM, Hitachi S-5000) and transmission electron microscope (TEM, FEI

TECNAI G^2) equipped with selected area electron diffraction (SAED) and energy dispersed X-ray detector (EDX) were applied for the detailed microstructure information. The SEM and TEM samples were prepared by depositing few droplets of the nanoparticle suspension onto the amorphous carbon coated copper grids, which were dried under argon atmosphere. The surface area measurements were performed by N_2 adsorption at liquid N_2 temperature using automatic volumetric adsorption equipment (Belsorp II). ^{15}N NMR spectra were recorded on a JEOL JNM-AL400 spectrometer at an operating frequency of 40.40 MHz. Liquid samples were contained in 5.0-mm-o.d. sample tubes, in which coaxial inserts containing CD_3CN (^{15}N, δ -134.00 ppm) as an external reference and a lock were placed. XPS analysis was carried out on a Shimadzu ESCA-3400 X-ray photoelectron spectrometer using an Mg Kα source (10 kV, 10 mA). The Ar sputtering experiments were carried out under the conditions of background vacuum 3.2×10^{-6} Pa, sputtering acceleration voltage 1 kV.

Preparation of $Ni_{0.95}Ir_{0.05}$-B, $Ni_{0.90}Ir_{0.10}$-B, $Ni_{0.75}Ir_{0.25}$-B, $Ni_{0.60}Ir_{0.40}$-B, $Ni_{0.50}Ir_{0.50}$-B and $Ni_{0.25}Ir_{0.75}$-B nanocatalysts. To a 2.0 mL aqueous suspension of $NiCl_2 \cdot 6H_2O$ (0.045 g) and CTAB (0.100 g), 500 μL of H_2IrCl_6 (0.02 M) were added and the light-yellow suspension was subsequently sonication and stirring for 5 min. The resulting homogenous suspension was heated at 50 °C in a water bath, leading to the appearance of a bright orange suspension. The suspension was cooled to room temperature, to which a 1.5 mL aq. $NaBH_4$ (0.35 M) solution was added dropwise. The content of the flask is vigorously shaked for 5 min, resulting in the generation of $Ni_{0.95}Ir_{0.05}$-*B* nanocatalyst as a black suspension, which was used for the catalytic reaction. $Ni_{0.90}Ir_{0.10}$-*B*, $Ni_{0.75}Ir_{0.25}$-*B*, $Ni_{0.60}Ir_{0.40}$-*B*, $Ni_{0.50}Ir_{0.50}$-*B* and $Ni_{0.25}Ir_{0.75}$-*B* nanocatalysts were prepared by using 0.008

and 0.043 g, 0.020 and 0.036 g, 0.032 and 0.028 g, 0.041 and 0.024 g, and 0.061 and 0.012 g of H_2IrCl_6 and $NiCl_2{\cdot}6H_2O$, respectively, by following the above procedure for $Ni_{0.95}Ir_{0.05}$-*B* nanocatalyst.

Preparation of $Ni_{0.95}Ir_{0.05}$-C and $Ni_{0.90}Ir_{0.10}$-C nanocatalysts. An analogous synthetic procedure was followed as above to prepare $Ni_{0.95}Ir_{0.05}$-*C* and $Ni_{0.90}Ir_{0.10}$-*C* by using CTAC in place of CTAB.

Preparation of the physical mixture of Ni and Ir nanocatalysts. Separately prepared Ni and Ir nanocatalysts were mixed together in the ratio of 95 mol% Ni and 5 mol% Ir.

Preparation of CTAB stabilized $M_{0.95}Ir_{0.05}$ (M = Fe, Co and Cu) nanocatalysts. The $M_{0.95}Ir_{0.05}$-*B* (M = Fe, Co, Cu) nanocatalysts were synthesized using the similar method as for the $Ni_{0.95}Ir_{0.05}$-*B* nanocatalyst using $FeCl_2{\cdot}4H_2O$ (0.038 g), $CoCl_2{\cdot}6H_2O$ (0.045 g) and $CuCl_2$ (0.026 g), respectively, in place of $NiCl_2{\cdot}6H_2O$.

Catalytic hydrous hydrazine decomposition experiments. Catalytic reactions were carried out at room temperature using a two-necked round bottom flask with one of the flask openings connected to a gas burette and another for the introduction of hydrazine monohydrate. Catalytic decomposition reaction of hydrazine for the release of hydrogen (along with nitrogen) was initiated by stirring the mixture of hydrazine monohydrate (0.1 mL, 1.97 mmol), which was introduced by using a syringe to the reaction flask containing the 4.0 mL aqueous suspension of the nanocatalysts (catalyst/hydrazine molar ratio 1/10). The gases released during the reaction was passed through a trap containing

1.0 M hydrochloric acid to ensure the absorption of ammonia, if produced, of which the volume was monitored using the gas burette.

Characterization of nanocatalysts. NiIr nanocatalysts were collected by centrifugation (15000 rpm, 10 min, 298 K) and were washed twice with 5.0 mL of water and 5.0 mL of ethanol. The nanoparticles were washed by acetone and dried under vacuum at room temperature for 8 h before characterisation by SEM, TEM, XPS and powder XRD.

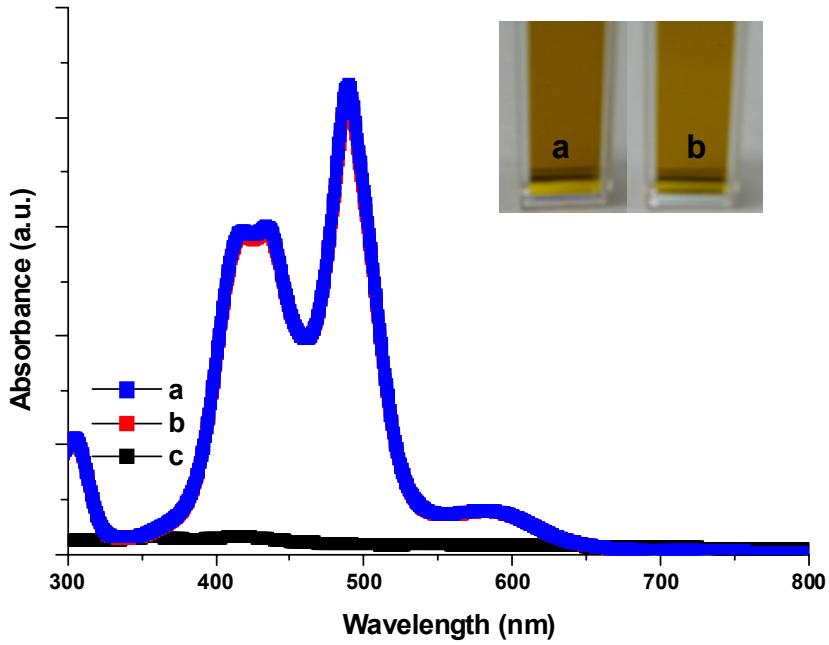

Fig. S1 UV-vis absorption spectra after (a) the addition of aqueous solutions of the mixture of Ni^{2+} and Ir^{4+} salts, (b) heating the solution (a) for 5 min at 50 °C (inset shows the colours observed for (a) and (b)), (c) reduction of the solution (b) by $NaBH_4$ for the preparation of surfactant free $Ni_{0.95}Ir_{0.05}$ nanocatalysts.

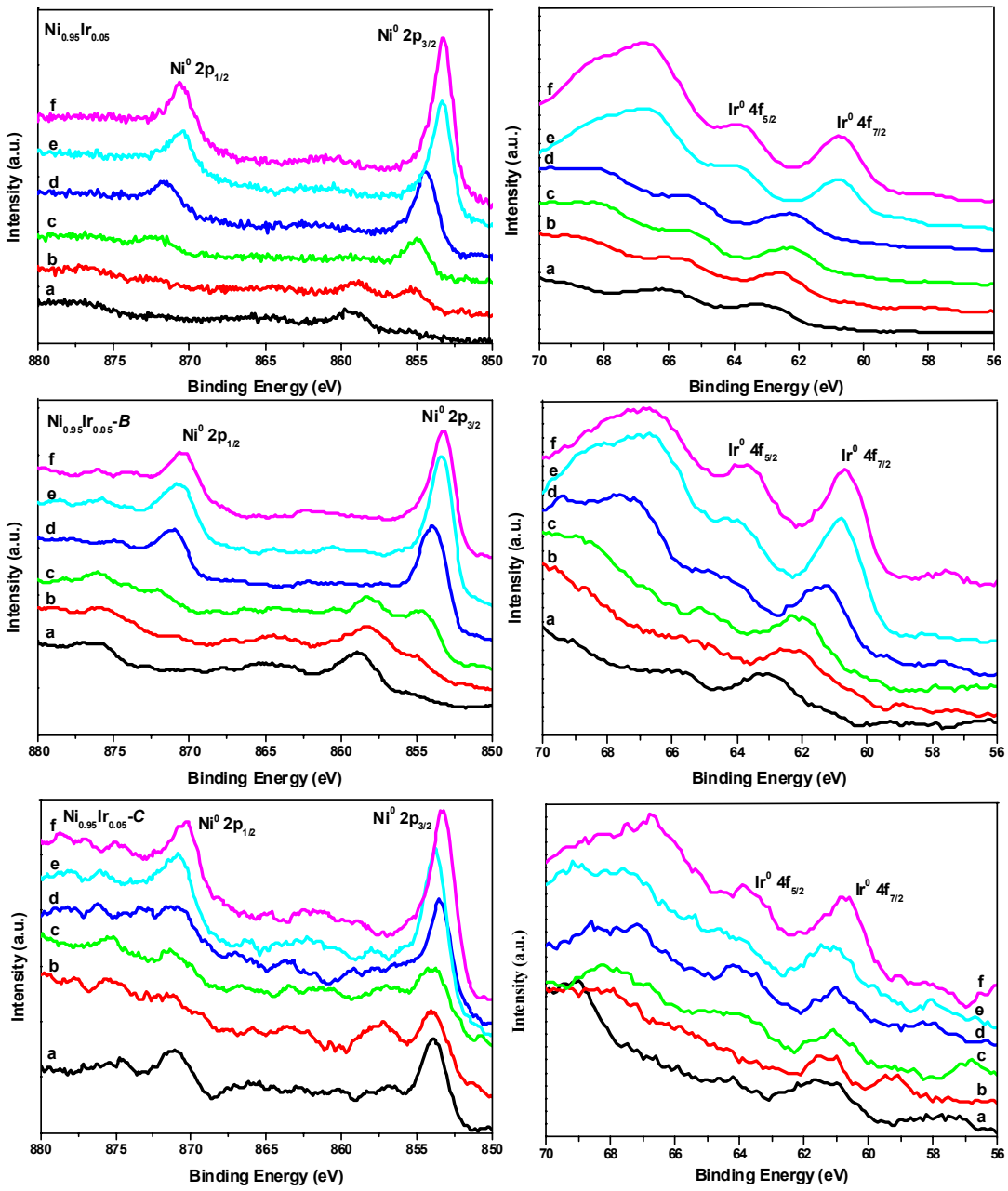

Fig. S2 The XPS profiles of Ni and Ir for the $Ni_{0.95}Ir_{0.05}$, $Ni_{0.95}Ir_{0.05}$-*B* and $Ni_{0.95}Ir_{0.05}$-*C* nanocatalysts (a) before and (b) 2, (c) 4, (d) 6, (e) 66 and (f) 186 min after argon sputtering.

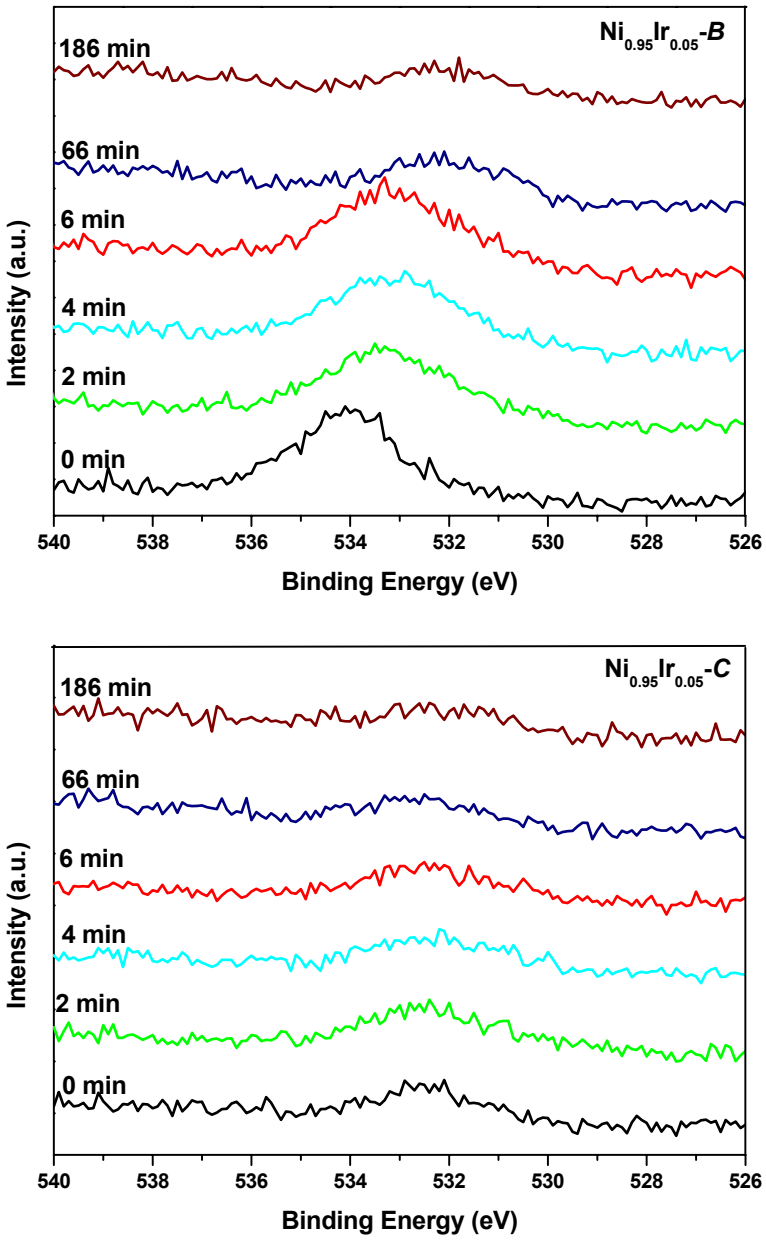

Fig. S3 The XPS profiles of oxygen 2p level for the $Ni_{0.95}Ir_{0.05}$-*B* and $Ni_{0.95}Ir_{0.05}$-*C* nanocatalysts.

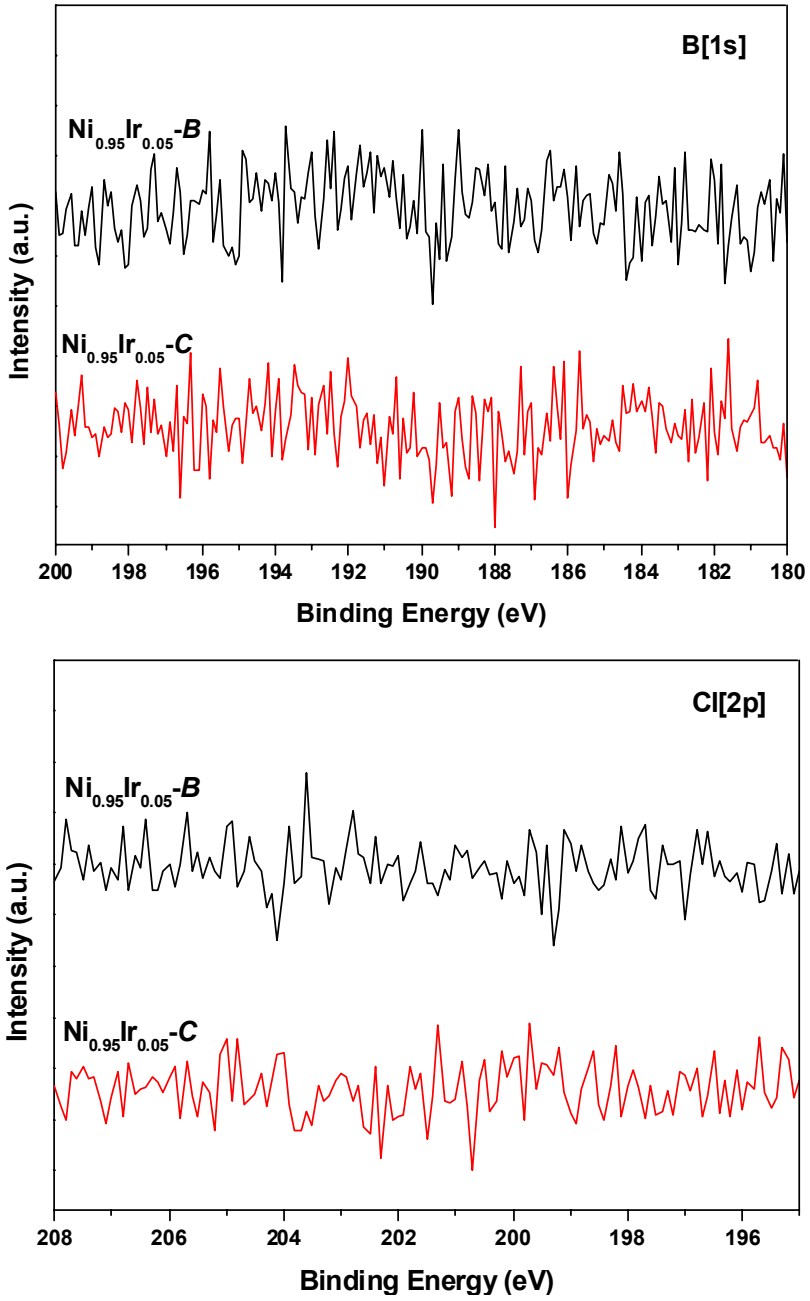

Fig. S4 The XPS profiles of the electron binding energy scanning ranges of B and Cl for the $Ni_{0.95}Ir_{0.05}$-*B* and $Ni_{0.95}Ir_{0.05}$-*C* nanocatalysts.

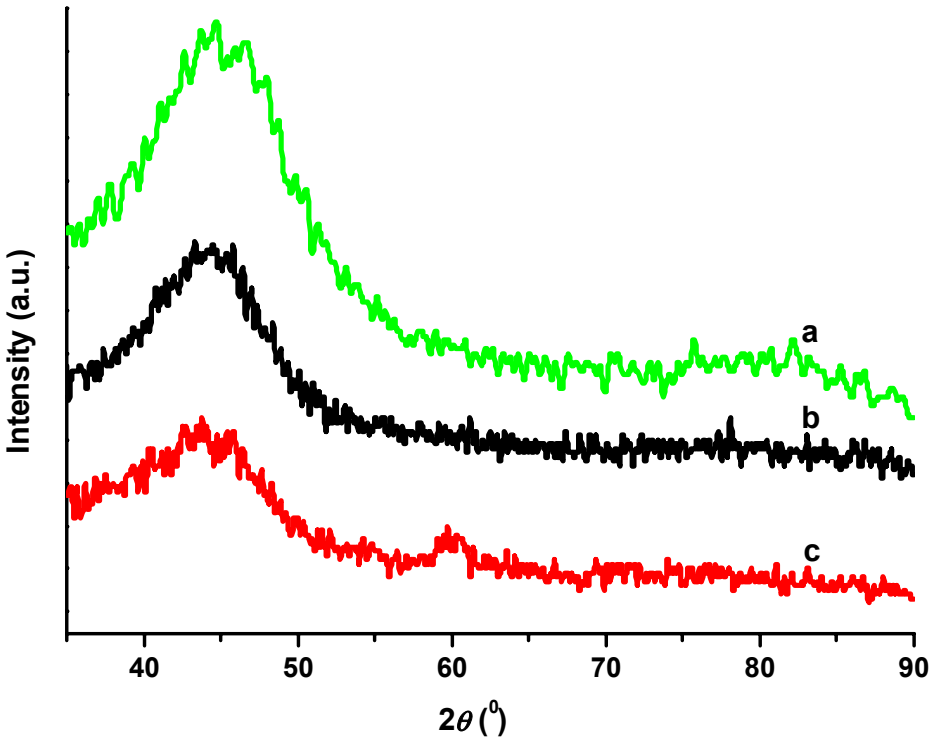

Fig. S5 Powder-XRD patterns of (a) $Ni_{0.95}Ir_{0.05}$, (b) $Ni_{0.95}Ir_{0.05}$-*B* and (c) $Ni_{0.95}Ir_{0.05}$-*C* nanocatalysts.

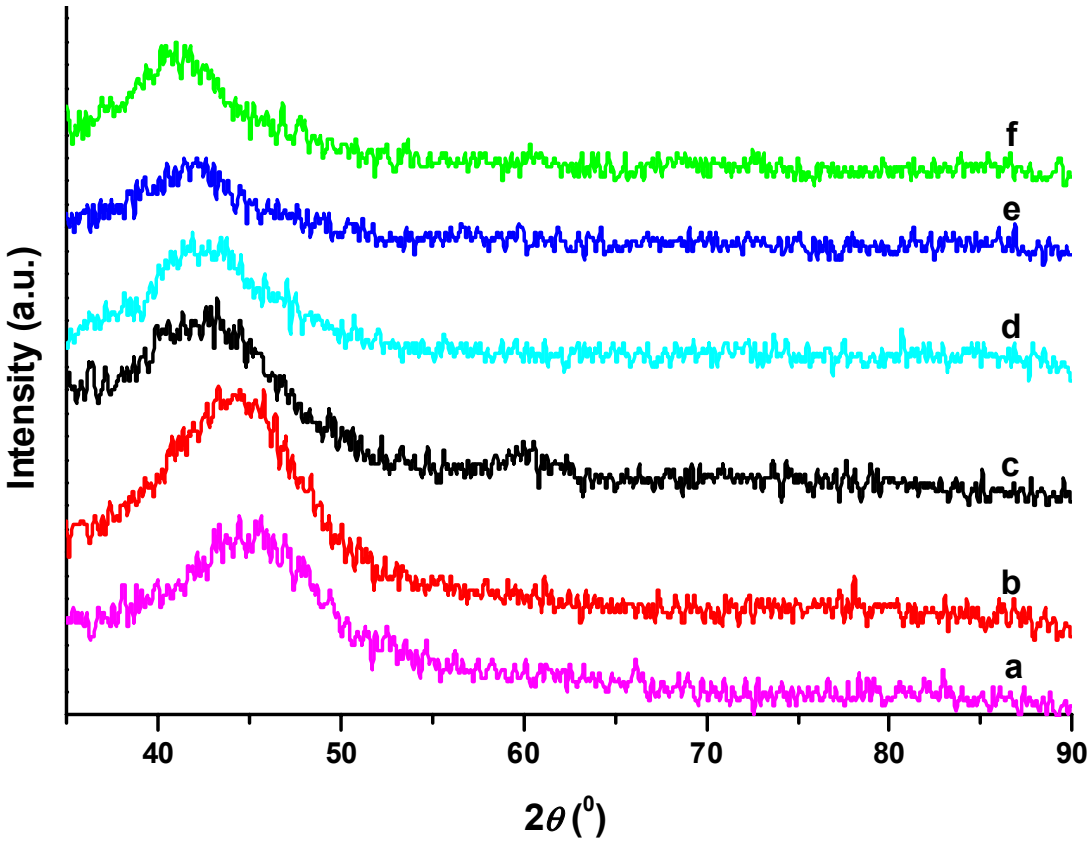

Fig. S6 Powder-XRD patterns of (a) $Ni_{0.99}Ir_{0.01}$-*B*, (b) $Ni_{0.95}Ir_{0.05}$-*B*, (c) $Ni_{0.90}Ir_{0.10}$-*B*, (d) $Ni_{0.75}Ir_{0.25}$-*B*, (e) $Ni_{0.60}Ir_{0.45}$-*B*, and (f) $Ni_{0.50}Ir_{0.50}$-*B* nanocatalysts.

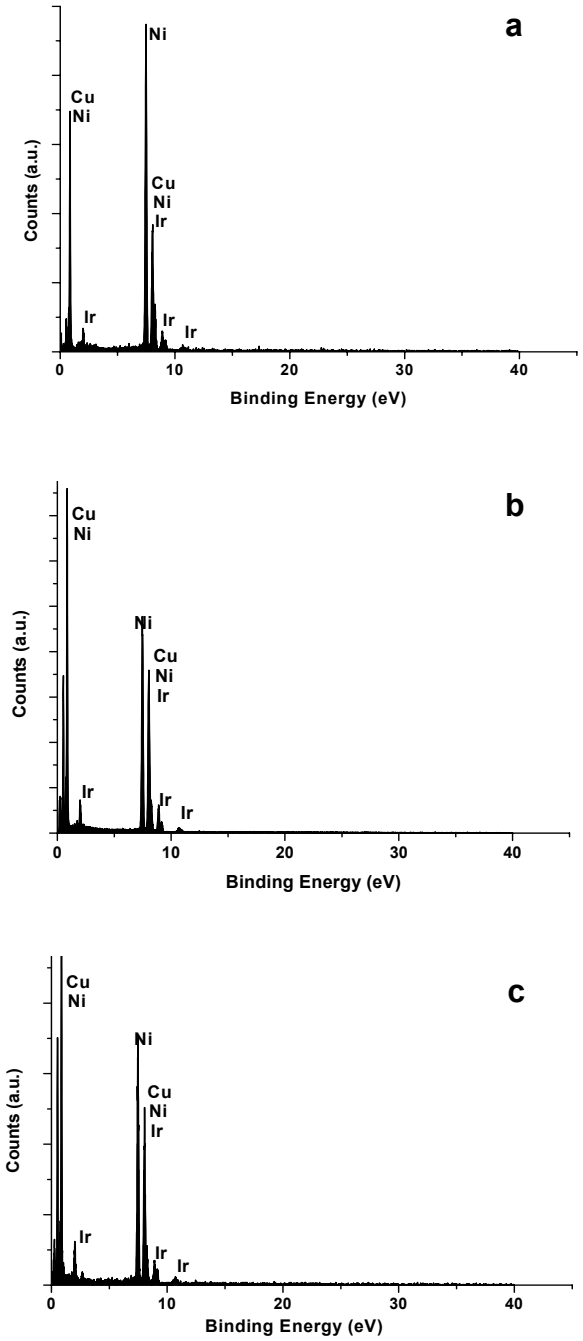

Fig. S7 EDX patterns for (a) $Ni_{0.95}Ir_{0.05}$, (b) $Ni_{0.95}Ir_{0.05}$-*B* and (c) $Ni_{0.95}Ir_{0.05}$-*C* nanoparticles.

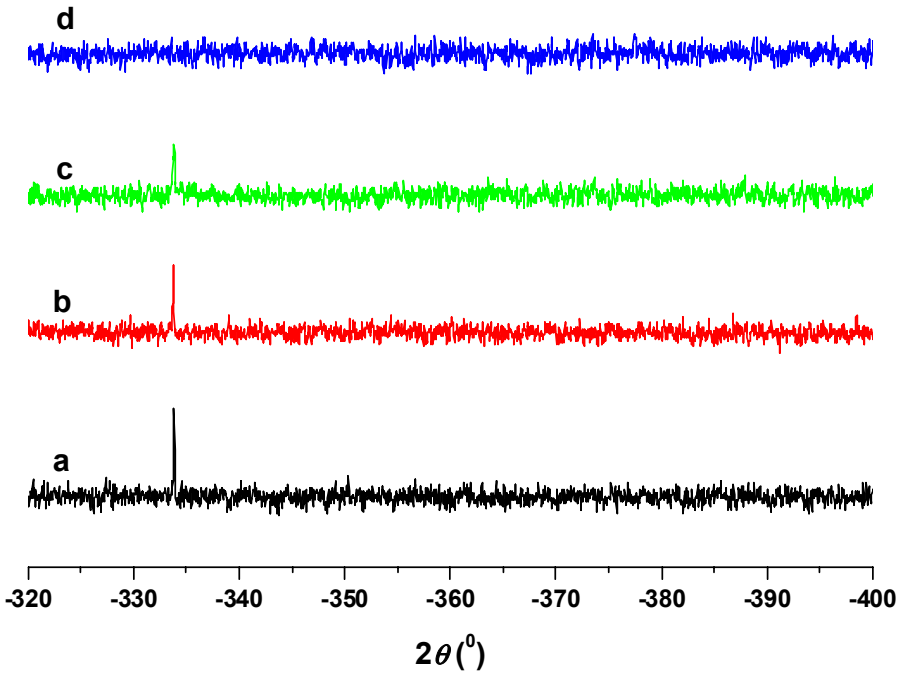

Fig. S8 ^{15}N NMR spectra (298 K, referenced to CD_3CN, δ -134.00 ppm) of (a) hydrous hydrazine (0.5 M), (b and c) after the reactions (2 h and 4 h, respectively) of (a) and (d) after the completion of hydrazine decomposition reaction of (a) over the $Ni_{0.95}Ir_{0.05}$-*B* nanocatalyst (catalyst/N_2H_4 molar ratio = 1:10) at 298 K.

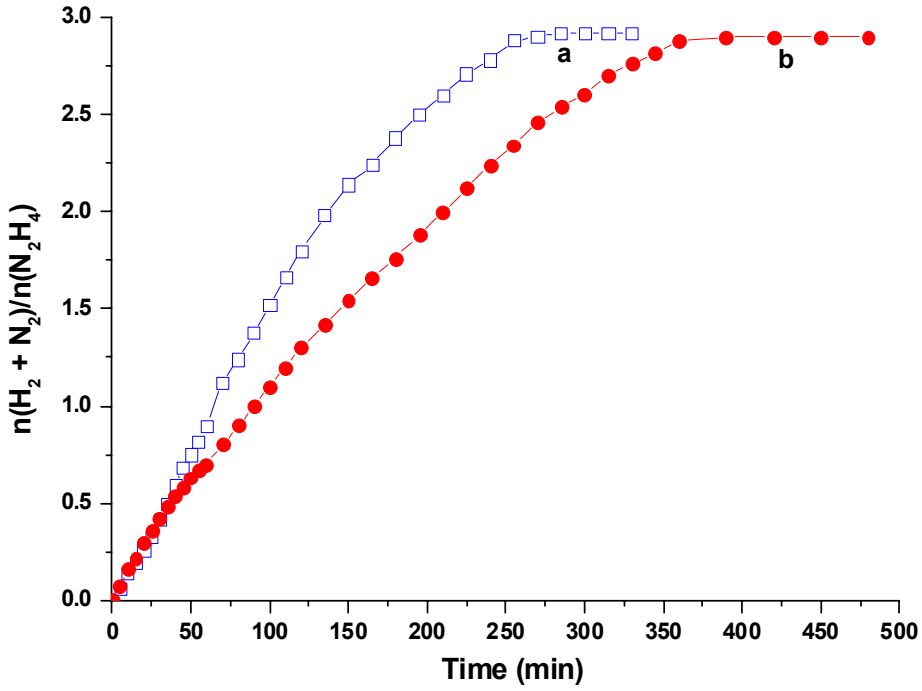

Fig. S9 Time course plots for decomposition of hydrous hydrazine (0.5 M) catalyzed over nickel-iridium alloy nanocatalysts (a) $Ni_{0.90}Ir_{0.10}$-*B* and (b) $Ni_{0.90}Ir_{0.10}$-*C* (catalyst/N_2H_4 molar ratio = 1:10) at 298 K.

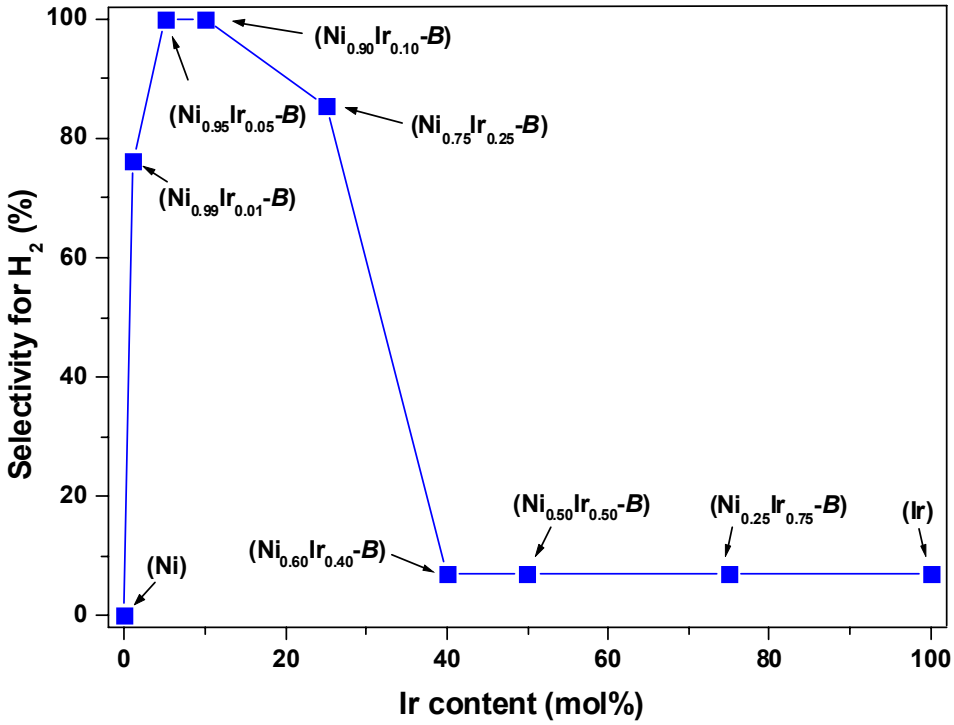

Fig. S10 Selectivity for hydrogen generation by decomposition of hydrous hydrazine (0.5 M) catalyzed by Ni, Ni_xIr_{1-x}-*B* (x = 0.95, 0.90, 0.75, 0.60, 0.50, and 0.25) and Ir nanocatalysts (catalyst/N_2H_4 molar ratio = 1:10) at 298 K.

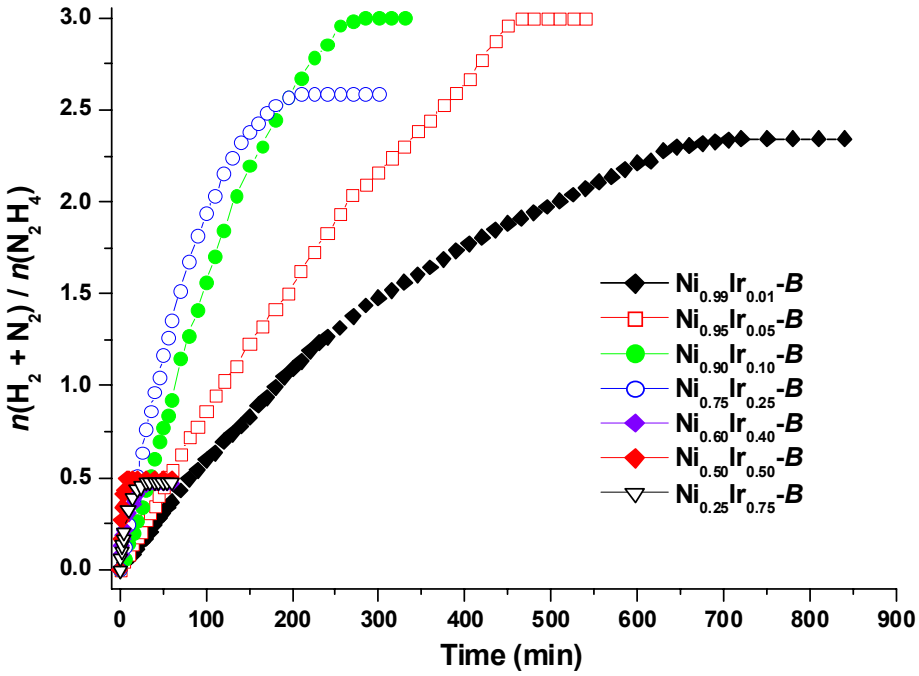

Fig. S11 Time course plots for hydrogen generation by decomposition of hydrous hydrazine (0.5 M) catalyzed by Ni_xIr_{1-x}-*B* (x = 0.95, 0.90, 0.75, 0.60, 0.50 and 0.25) nanocatalysts (catalyst/N_2H_4 molar ratio = 1:10) at 298 K.

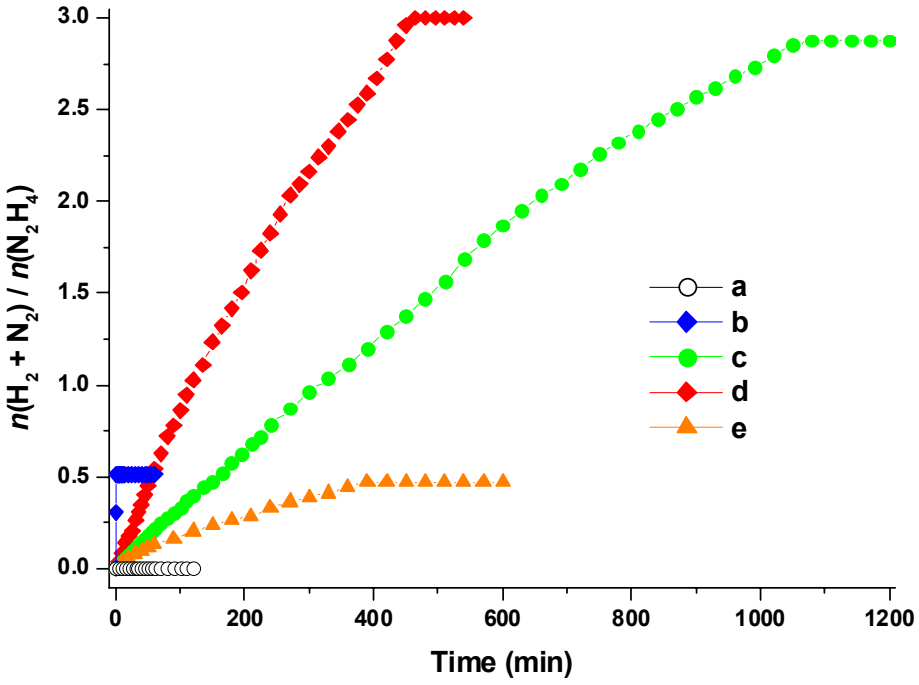

Fig. S12 Time course plots for decomposition of hydrous hydrazine (0.5 M) catalyzed over (a) Ni NPs, (b) Ir NPs, (c) $Ni_{0.95}Ir_{0.05}$, (d) $Ni_{0.95}Ir_{0.05}$-*B* and (e) the physical mixture of Ni and Ir NPs (catalyst/N_2H_4 molar ratio = 1:10) at 298 K.

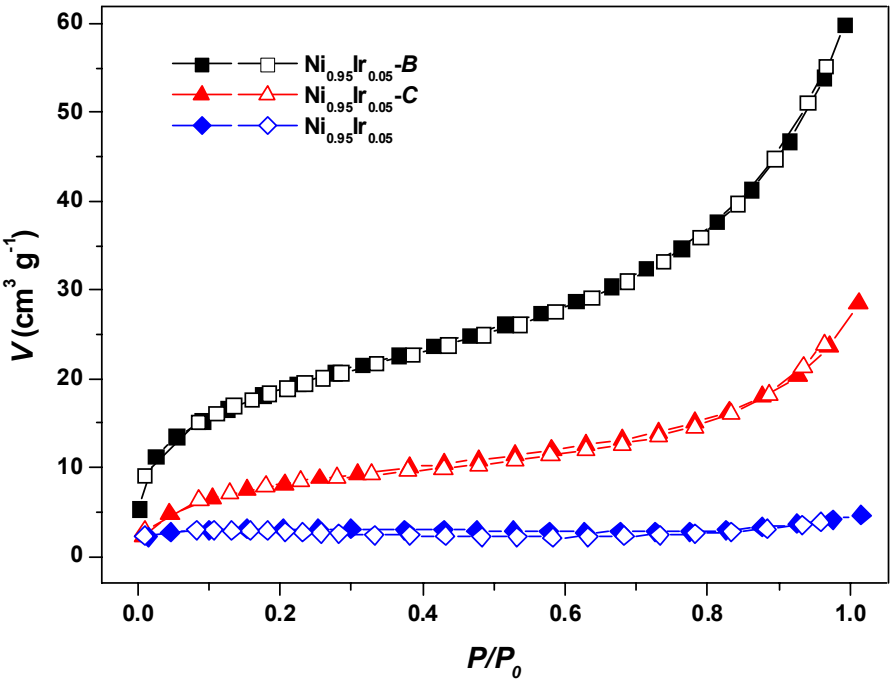

Fig. S13 Nitrogen adsorption-desorption isotherms of $Ni_{0.95}Ir_{0.05}$, $Ni_{0.95}Ir_{0.05}$-*B* and $Ni_{0.95}Ir_{0.05}$-*C* nanocatalysts at 77 K (P_0 = 1.0 atm).

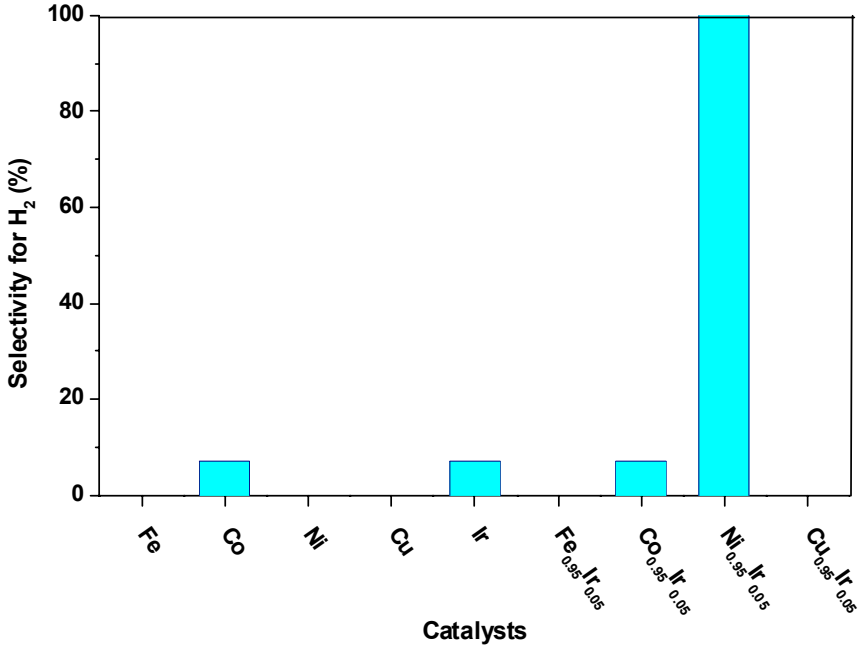

Fig. S14 Selectivity for hydrogen generation from decomposition of hydrous hydrazine (0.5 M) catalyzed over Fe, Co, Ni, Cu, Ir, $Fe_{0.95}Ir_{0.05}$, $Co_{0.95}Ir_{0.05}$, $Ni_{0.95}Ir_{0.05}$ and $Cu_{0.95}Ir_{0.05}$ (catalyst/N_2H_4 molar ratio = 1:10) nanocatalysts obtained in the presence of CTAB at 298 K.

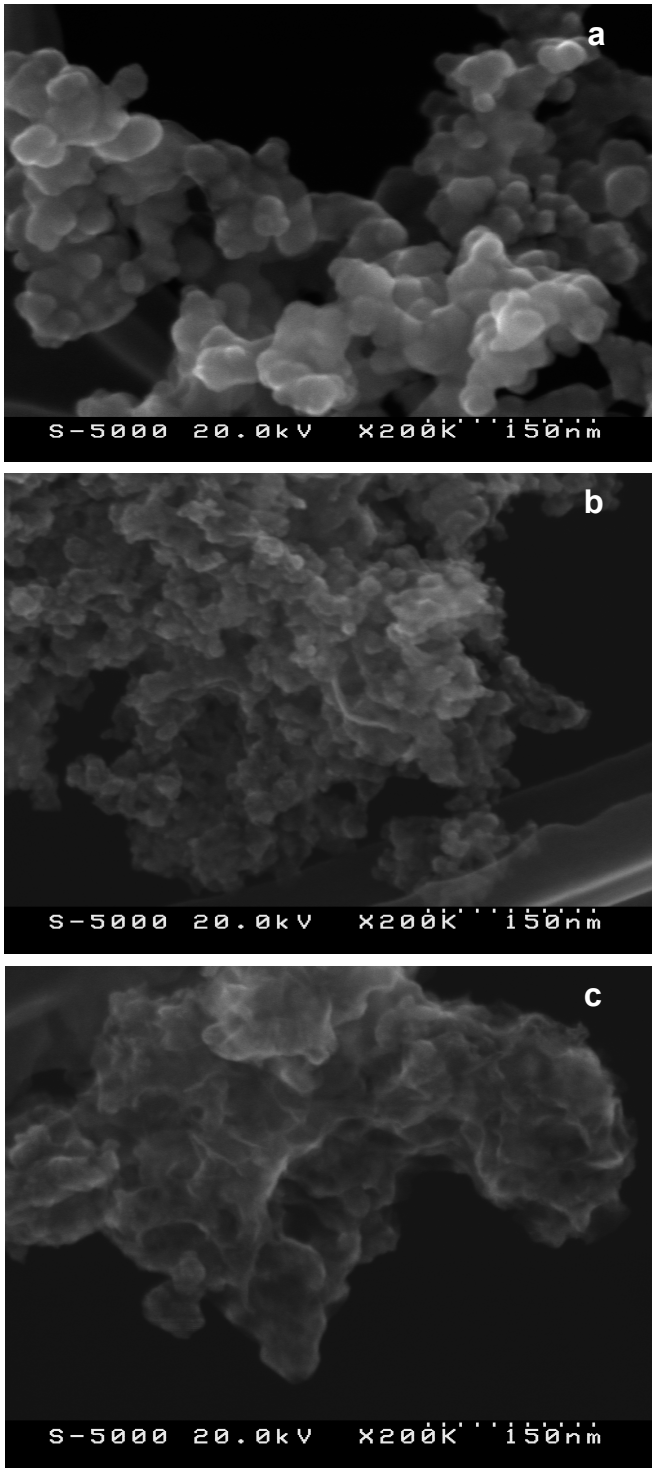

Fig. S15 SEM images of (a) $Ni_{0.95}Ir_{0.05}$, (b) $Ni_{0.95}Ir_{0.05}$-*B* and (c) $Ni_{0.95}Ir_{0.05}$-*C* nanocatalysts.